Ultrahigh resolution photoacoustic microscopy via transient absorption

Ryan L. Shelton and Brian E. Applegate*

Department of Biomedical Engineering, Texas A&M University, 337 Zachry Engineering Center, TAMU 3120, College Station, TX 77843, USA
**apple@tamu.edu*

Abstract: We have developed a novel, hybrid imaging modality, Transient Absorption Ultrasonic Microscopy (TAUM), which takes advantage of the optical nonlinearities afforded by transient absorption to achieve ultrahigh-resolution photoacoustic microscopy. The theoretical point spread function for TAUM is functionally equivalent to confocal and two-photon fluorescence microscopy, potentially enabling cellular/subcellular photoacoustic imaging. A prototype TAUM system was designed, built, and used to image a cross-section through several capillaries in the excised cheek pouch of a Syrian Hamster. The well-resolved capillaries in the TAUM image provided experimental evidence of the spatial resolution. These results suggest that TAUM has excellent potential for producing volumetric images with cellular/subcellular resolution in three dimensions deep inside living tissue.

OCIS codes: (110.5120) Photoacoustic imaging; (110.5125) Photoacoustics; (180.4315) Nonlinear microscopy.

References and links

1. K. Maslov, G. Stoica, and L. V. H. Wang, "In vivo dark-field reflection-mode photoacoustic microscopy," Opt. Lett. **30**(6), 625–627 (2005).
2. S. Hu, and L. V. Wang, "Photoacoustic imaging and characterization of the microvasculature," J. Biomed. Opt. **15**(1), 011101 (2010).
3. J. T. Oh, M. L. Li, H. F. Zhang, K. Maslov, G. Stoica, and L. V. Wang, "Three-dimensional imaging of skin melanoma in vivo by dual-wavelength photoacoustic microscopy," J. Biomed. Opt. **11**(3), 034032 (2006).
4. Y. S. Yang, S. Vaithilingam, H. T. J. Ma, S. Salehi-Had, O. Oralkan, B. T. Khuri-Yakub, and S. Guccione, "Development of Nanoparticle-Based Gold Contrast Agent for Photoacoustic Tomography," NSTI Nanotech 2008, Vol 1, Technical Proceedings 708–711, 1092 (2008).
5. G. Kim, S. W. Huang, K. C. Day, M. O'Donnell, R. R. Agayan, M. A. Day, R. Kopelman, and S. Ashkenazi, "Indocyanine-green-embedded PEBBLEs as a contrast agent for photoacoustic imaging," J. Biomed. Opt. **12**(4), 044020 (2007).
6. K. Maslov, H. F. Zhang, S. Hu, and L. V. Wang, "Optical-resolution photoacoustic microscopy for in vivo imaging of single capillaries," Opt. Lett. **33**(9), 929–931 (2008).
7. K. Maslov, G. Ku, and L. V. Wang, "Photoacoustic microscopy with submicron resolution," in (SPIE, 2010), 75640W.
8. C. E. Crespo-Hernández, B. Cohen, and B. Kohler, "Base stacking controls excited-state dynamics in A.T DNA," Nature **436**(7054), 1141–1144 (2005).
9. B. E. Applegate, and J. A. Izatt, "Molecular imaging of endogenous and exogenous chromophores using ground state recovery pump-probe optical coherence tomography," Opt. Express **14**(20), 9142–9155 (2006).
10. B. E. Applegate, C. Yang, and J. A. Izatt, "Theoretical comparison of the sensitivity of molecular contrast optical coherence tomography techniques," Opt. Express **13**(20), 8146–8163 (2005).
11. C. Y. Dong, P. T. C. So, C. Buehler, and E. Gratton, "Spatial resolution in scanning pump-probe fluorescence microscopy," Optik (Stuttg.) **106**, 7–14 (1997).
12. C. J. R. Sheppard, and M. Gu, "Image-Formation in 2-Photon Fluorescence Microscopy," Optik (Stuttg.) **86**, 104–106 (1990).
13. C. M. W. Daft, G. A. D. Briggs, and W. D. O'Brien, Jr., "Frequency dependence of tissue attenuation measured by acoustic microscopy," J. Acoust. Soc. Am. **85**(5), 2194–2201 (1989).
14. J. Squier, and M. Muller, "High resolution nonlinear microscopy: A review of sources and methods for achieving optimal imaging," Rev. Sci. Instrum. **72**(7), 2855–2867 (2001).

#129372 - $15.00 USD Received 1 Jun 2010; revised 12 Aug 2010; accepted 14 Aug 2010; published 23 Aug 2010

15. R. L. Shelton, and B. E. Applegate, "Off-axis photoacoustic microscopy," IEEE Trans. Biomed. Eng. **57**(8), 1835–1838 (2010).
16. G. Ku, K. Maslov, L. Li, and L. V. Wang, "Photoacoustic microscopy with 2-microm transverse resolution," J. Biomed. Opt. **15**(2), 021302 (2010).

1. Introduction

Photoacoustic microscopy (PAM) [1] is a recently developed high-resolution, absorption-contrast imaging modality primarily applied to imaging in turbid media, such as tissue. Typical chromophore targets include hemoglobin [2], melanin [3], gold nanoparticles [4], and dyes [5]. The weak attenuation of acoustic emission permits high-resolution imaging in tissue up to several millimeters deep [1]. Recent advances have significantly improved the lateral spatial resolution by optically limiting the excitation volume [6] enabling submicron lateral resolution [7]. While the lateral resolution is optically limited, the axial resolution is limited by the bandwidth of the ultrasonic detector, estimated to be ~15 μm (75 MHz detector) in [6], yielding a highly asymmetric voxel.

Higher axial resolution and a more symmetric voxel would be advantageous for high-resolution imaging. The axial resolution is linearly dependent on the transducer bandwidth. An axial resolution of 1.5 μm would require a 1 GHz bandwidth detector. Imaging with such high acoustic frequencies poses several problems including detector construction, acoustic dispersion and acoustic attenuation. A 300 MHz acoustic wave is attenuated at a rate of ~20 dB/mm in water and ~80 dB/mm in tissue, which would practically limit the imaging depth to ~100 μm [6]. Simply increasing the detector bandwidth does not appear to be an effective approach to a more symmetric voxel.

Here we propose and demonstrate for the first time an alternate approach, Transient Absorption Ultrasonic Microscopy (TAUM), that uses optical nonlinearities to optically limit the spatial resolution in *both* the axial and lateral dimensions. The approach effectively fuses pump-probe absorption spectroscopy with photoacoustic microscopy. Pump-probe absorption spectroscopy is a well-established tool in molecular physics for measuring the spectrum and dynamics of molecular species that exhibit low fluorescence quantum yield. In fact, the relaxation dynamics of DNA after absorption of UV light has recently been studied using pump-probe absorption spectroscopy [8].

Pump-probe spectroscopy inherently measures pump-induced changes in the attenuation of the probe. On a molecular level, interaction with the pump radiation induces changes in molecular state populations. The probe interrogates these population changes and reports via a pump dependent change in the probe attenuation. If the pump is amplitude modulated, the modulation will be transferred to the probe. Nominally, the probe must be delayed in time relative to the pump. If the probe signal is measured as a function of the interpulse pump-probe delay, the signal should map out an exponential that decays at a characteristic time corresponding to the time it takes the molecular state population to return to equilibrium. This time is often referred to as the ground state recovery time of the molecule.

The pulsed laser induced photoacoustic emission, $p(r,t)$, from a molecular absorber may be written as

$$p(r,t) = \sigma N_1 F \kappa(r,t), \tag{1}$$

where σ is the absorption cross-section, N_1 is the ground state population density, F is the laser fluence, and $\kappa(r,t)$ is a term describing the space and time-dependence of the pressure profile, as well as the material properties of the absorber. This equation is more traditionally expressed in terms of the absorption coefficient, μ_a, where $\mu_a = \sigma N_1$. As noted above, the pump will change the population, N_1, thereby changing the photoacoustic emission from the probe. In order to illustrate the underlying physics we will utilize a simple two-state system, for which we have previously derived the relevant equations governing the time dependent state populations [9,10].

#129372 - $15.00 USD Received 1 Jun 2010; revised 12 Aug 2010; accepted 14 Aug 2010; published 23 Aug 2010

Consider a two-state molecular system isolated in an ideal solvent that quenches the excited state with a time constant τ resulting in photoacoustic emission. If the pump pulse duration is much less than τ and the transition is far from saturation, the population of the ground state after interacting with a pump pulse is given by

$$N_1 = N_1^0\left(1-\frac{\sigma\lambda_{pu}F_{pu}}{hc}\exp\left(-t_d/\tau\right)\right), \tag{2}$$

where $N_1{}^0$ is the initial (before interacting with pump radiation) ground state population, λ_{pu} is the pump wavelength, F_{pu} is the pump fluence, h is Planck's constant, c is the speed of light, and t_d is the interpulse delay between the pump and probe. The pump-probe signal may be extracted by taking the difference in the photoacoustic emission amplitude with pump on and off, i.e.

$$\Delta p(r,t) = \sigma N_1^0\left(\frac{\sigma\lambda_{pu}F_{pu}}{hc}\exp\left(-t_d/\tau\right)\right)F_{pr}\kappa(r,t). \tag{3}$$

Note the quadratic dependence on fluence; a property shared with other two-photon microscopy techniques.

Equation (3) is dependent of two molecular-specific physical properties, σ and τ. The wavelength dependence of the absorption coefficient, σ, may be measured by recording the signal as a function of pump or probe wavelength. Similarly, the state recovery time, τ, may be measured by recording the signal as a function of interpulse delay (t_d) and fitting the result to an exponential decay. Both properties may be used to gain specificity for the target molecule.

The spatial resolution of TAUM is governed by the pump-probe interaction, rather than the ultrasonic transducer specifications. The point spread function (PSF) resulting from the overlap of the pump and probe beams has been derived previously by Dong, et al. [11],

$$PSF_{TAUM} = I(r,z)I'(r',z'), \tag{4}$$

where the prime indicates the pump beam, the molecular transition is assumed to be far from saturation, and the light intensity profile is defined as

$$I(r,z) = \left|2\int_0^1 J_0\left(kr\sin\alpha,\rho\right)\exp\left(\frac{1}{2}i4kz\sin^2\left(\frac{\alpha}{2}\right)\rho^2\right)d\rho\right|^2, \tag{5}$$

where r and z are the radial and axial coordinates, respectively, k is the wavenumber, ρ is the radial dimension in the polar coordinate system, and $\sin\alpha$ is the numerical aperture of the objective lens. If the pump and probe beams share the same wavelength, then Eq. (4) simplifies to $PSF_{TAUM} = I(r,z)^2$, which is equivalent to the PSF for confocal microscopy and two-photon fluorescence microscopy [12]. TAUM should therefore be capable of subcellular, photoacoustic imaging in three dimensions. Just as in two-photon fluorescence microscopy, as the transition approaches saturation the resolution is degraded. If the transition is saturated along the entire depth of focus, there will be no sectioning from the pump-probe overlap. If the molecular absorber is photobleached there will be a reduction in total signal, however, the resolution will be unaltered.

A significant advantage of this pump-probe technique is that it is freed of any frequency restraints imposed on the transducer by axial resolution requirements. Transducers with center frequencies of 50 – 100 MHz are commonly used in photoacoustic microscopy to optimize the resolution in the axial dimension. The downside to increasing the transducer frequency is that higher frequency acoustic waves are much more attenuated in tissue than lower frequency

#129372 - $15.00 USD Received 1 Jun 2010; revised 12 Aug 2010; accepted 14 Aug 2010; published 23 Aug 2010

waves, resulting in much lower effective imaging depths for high frequency transducers. A 5 MHz acoustic wave is attenuated 200 times less in tissue than a 100 MHz acoustic wave [13]. In order to get an axial resolution of 1 μm (the theoretical optical resolution in the experiments described below), a 1.5 GHz transducer would have to be used. At these high frequencies, the attenuation of the acoustic waves in tissue is ~20,000 times greater. Since the resolution in TAUM does not rely on the detector bandwidth, 1 μm resolution may be achieved even with low frequency ultrasonic transducers.

2. Methods and materials

A prototype TAUM system has been built in order to evaluate the potential of TAUM for high-resolution imaging. A schematic diagram of the system is shown in Fig. 1. The excitation source was a Q-switched, 1064 nm, DPSS laser (1Q 532-2, Crylas), frequency doubled to 532 nm with pulse duration of 1.3 ns and a maximum repetition rate of 10 kHz. The output of the laser was directed to a beam splitter, where the forward propagated light formed the probe and the reflected light formed the pump. The pump and probe passed through either side of a dual frequency optical chopper before being recombined with a second beam splitter after the probe had been delayed ~1 ns relative to the pump. The ground state recovery time for hemoglobin at a wavelength of 532nm is ~9 ns [9]. A delay of 1 ns was chosen as a value that was geometrically convenient for our system's implementation of the dual frequency chopper, but short enough to ensure sufficient population in the excited state when the probe is incident on the sample. The transient absorption signal is linearly dependant on the population of the probed energy state; therefore, the interpulse delay time is very important for optimal signal-to-noise. The recombined beam was passed through a beam expander formed by L1 and L2, then focused onto the sample through one of two water immersion microscope objectives (NIR APO 40X/.80 3.5 mm WD, CFI W Plan Fluor 10X/.30 3.5 mm WD, Nikon), depending on the experiment. The photoacoustic signals were collected using one of two focused ultrasonic transducers (V310-SU, V322-SU, Olympus NDT. The V310 is a 6 MHz center frequency transducer with a 6 mm element size, 80% (–6 dB) bandwidth, and a numerical aperture of 0.23. The V322 is a 25 MHz center frequency transducer with a 6 mm element size, 60% (–6 dB) bandwidth, and a numerical aperture of 0.16. For each experiment, the ultrasonic transducer was fixed at a 45° angle to the optical axis. The resulting photoacoustic signals from the transducer were then amplified through two radio frequency amplifiers (ZFL-500LN, Mini-Circuits), providing ~26 dB total amplification. The amplified signal was collected and digitized with a high-speed digital oscilloscope (DPO-7254, Tektronix), then processed and stored using a custom Labview GUI.

#129372 - $15.00 USD Received 1 Jun 2010; revised 12 Aug 2010; accepted 14 Aug 2010; published 23 Aug 2010

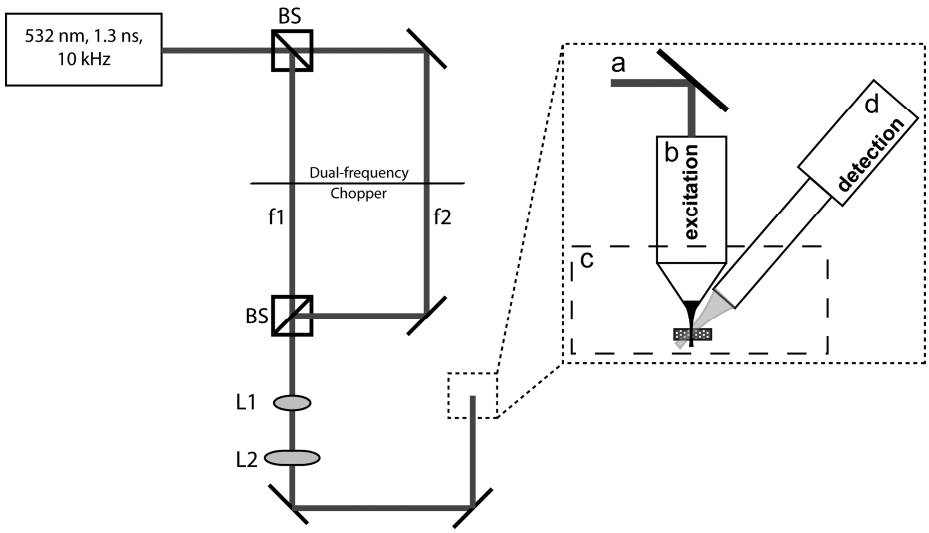

Fig. 1. Schematic diagram of the prototype TAUM system. f1 and f2 are the modulation frequency of the pump and probe, respectively, as induced by a dual frequency optical chopper. L1 and L2 form a beam expander to fill the aperture of the objective (b). The sample is placed in a water bath (c) for acoustic coupling. A 6 or 25 MHz center frequency ultrasonic transducer serves as the detector (d).

The 6 MHz transducer was used for the preliminary studies because that is what was available at the time of the experiment. The 25 MHz transducer was later acquired and used for the subsequent experiments due to the increased bandwidth, leading to the collection of more harmonic side bands (described below). The center frequency of the transducer is of little consequence to the TAUM signal; however, the bandwidth, which is ultimately limited by the center frequency of the transducer, determines the number of harmonics collected. There is some advantage in matching the transducer center frequency and the laser repetition rate, since this would concentrate the signal power in fewer harmonics over the detectors bandwidth. However, this strategy is only practical for MHz repetition rate laser sources.

While Eq. (3) plainly illustrates the source of the pump-probe signal, simply calculating the difference in the temporal trace of the photoacoustic emission from an “on” and “off” experiment is prone to a number of noise and background sources more efficiently avoided in the frequency domain. For instance, the pump and probe photoacoustic signals are nearly completely overlapped in the time-domain making it impractical to detect pump-induced changes in the time-domain probe signal. However, if we frequency encode the pump and probe at different frequencies, they will not overlap in the frequency-domain. In order to implement frequency domain signal collection, the signal is frequency-encoded via amplitude modulation of the pump and probe beams using a dual frequency optical chopper (3501, Newport Corp.) with a 42/30 ratio blade, capable of up to 4.48 kHz amplitude modulation. The transient absorption signal will then appear at the sum and difference frequencies of the pump and probe modulation, which may be readily extracted in the frequency domain.

The optical chopper imposes a square wave modulation on the pulse train of the laser. A square wave is well represented by a Fourier series containing only odd harmonics of the square wave frequency. Similarly, the pulsed source can be treated mathematically as a Fourier series, although all of the harmonics have a finite intensity. In both cases, the most intense band is the fundamental. Therefore, it is reasonable to derive the harmonic content of our signal by truncating the Fourier series after the first term. Moreover, by imposing a cosinusoidal modulation on the pump and probe fluence, the total time domain signal for the two-state system will be

#129372 - $15.00 USD Received 1 Jun 2010; revised 12 Aug 2010; accepted 14 Aug 2010; published 23 Aug 2010

$$p(r,t) = \sigma N_1^0 F_{pu}\left(\frac{1+\cos(\omega_{pu}t)}{2}\right)\left(1-\exp\left(-t_d/\tau\right)\right)\kappa'(r,t) + \sigma N_1^0\left(1-\frac{\sigma\lambda_{pu}F_{pu}\left(\frac{1+\cos(\omega_{pu}t)}{2}\right)}{hc}\exp\left(-t_d/\tau\right)\right)F_{pr}\left(\frac{1+\cos(\omega_{pr}t)}{2}\right)\kappa(r,t), \quad (6)$$

where the first term is photoacoustic emission due to the pump and the second term is photoacoustic emission due to the probe. The pump (ω_{pu}) and probe (ω_{pr}) modulation frequencies are slow compared to the laser repetition rate. If we record $p(r,t)$ over a large number of laser pulses with an ideal pressure transducer at r_0 and Fourier transform into the frequency domain, then

$$P(r_0,\omega) = \mathrm{K}(r_0,\omega)\sum_{n=0}^{\infty}\begin{pmatrix} A\delta(n\omega_l) + B\delta(n\omega_l \pm \omega_{pu}) \\ +C\delta(n\omega_l \pm \omega_{pr}) + D\delta(n\omega_l \pm (\omega_{pu} \pm \omega_{pr})) \end{pmatrix}, \quad (7)$$

where ω_l is the laser repetition frequency, K (r,ω) is the Fourier transform of $\kappa(r,t)$ which is notoriously broadband and resembles a log-normal distribution, the A, B, and C, coefficients are due to single photon photoacoustic emission and D is due to the pump-probe interaction, which for the two-state system described above is proportional to Eq. (3) divided by $\kappa(r,t)$. Eight sidebands are associated with every harmonic (n) of the laser repetition frequency. A real pressure transducer will attenuate and bandpass $P(r_0,\omega)$. Thus, the TAUM signal is the piecewise integral of all of the D sidebands in the attenuated and bandpassed $P(r_0,\omega)$.

Figure 2 is a simulation of Eq. (7) for n = 1 assuming a 10 kHz laser repetition rate, a pump modulation of 1 kHz and a probe modulation of 0.7 kHz. Panel A is the signal with no modulation of the pump and probe. Panel B is the signal with the pump and probe modulated, but no pump-probe interaction. Panel C includes the bands due to the pump-probe interaction. The signals due to pump, probe, and the pump-probe interaction may be clearly delineated in the frequency domain.

#129372 - $15.00 USD Received 1 Jun 2010; revised 12 Aug 2010; accepted 14 Aug 2010; published 23 Aug 2010

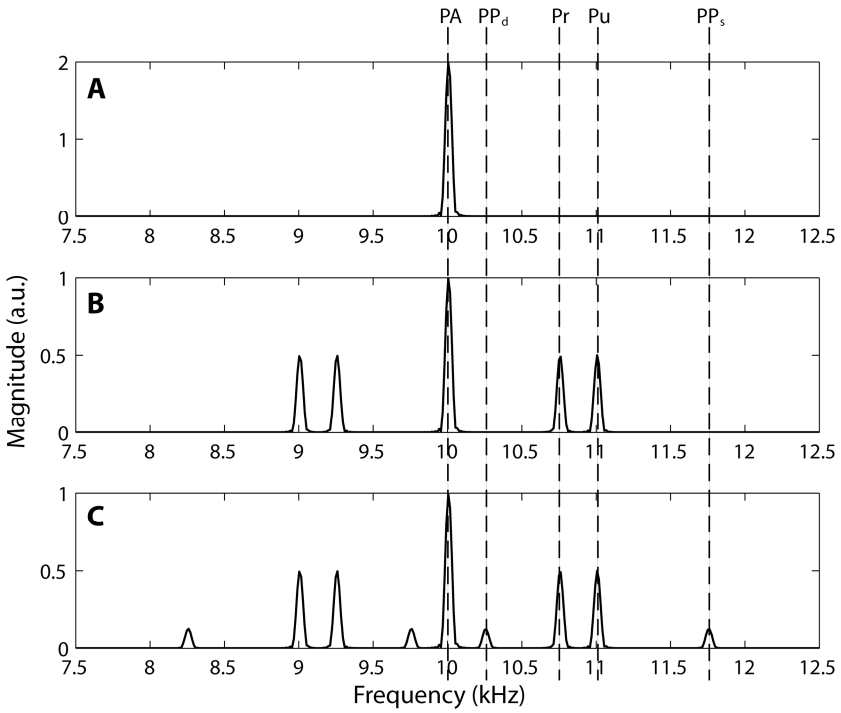

Fig. 2. Simulation of $P(r_0,\omega)$ with n = 1, Eq. (7). Panel A shows the resulting frequency band due to single photon photoacoustic emission (PA) at the laser repetition rate of 10 kHz (ω_l). Panel B includes the amplitude modulation of the pump (Pu) and probe (Pr) fluence, which adds beat frequencies of the pump and probe at 1 kHz ($\pm\ \omega_{pu}$) and 0.7 kHz ($\pm\ \omega_{pr}$), respectively to the 10 kHz band. All bands are due to single photon photoacoustic emission. Panel C includes the pump-probe interaction (coefficient *D*, Eq. (7), which induces sidebands at the sum (PP$_s$), 1.7 kHz ($\pm\ (\omega_{pu} + \omega_{pr})$) and difference (PP$_d$), 0.3 kHz ($\pm\ (\omega_{pu} - \omega_{pr})$) of the pump and probe modulation.

In practice, the time domain photoacoustic signal was recorded for 1000 sequential laser pulses with a window length of 2 μs using the *fast frame* function of the oscilloscope. The 98 μs of "dead" time between laser pulses was not recorded in order to reduce the record length. Nevertheless, transferring the record from the oscilloscope to PC for processing was the rate-limiting factor for imaging. The fast Fourier transform of the signal was then calculated. The sidebands [*D*, Eq. (7)] were integrated over their bandwidth and summed to get one TAUM pixel.

3. Results and discussion

As a preliminary experiment to test the sectioning capabilities of TAUM, a small drop of whole, human blood was injected between two 190 μm-thick glass coverslips, separated with 190 μm spacers. While there was likely refraction of the acoustic waves through the coverslips, no issues arose during the experiment to suggest this refraction to be problematic. After the blood had coagulated, axial depth scans were performed to obtain the axial profile of the sample with the imaging system.

For this lower-resolution experiment, the 0.3 NA objective was used to illuminate the sample. The back aperture of the lens was filled to produce a theoretical, diffraction-limited transverse resolution of 0.918 μm and axial resolution of 13.4 μm, given by the Rayleigh criteria described in [14]. The pulse energy at the sample surface was 180 nJ and 120 nJ in the pump and probe beams, respectively. The photoacoustic signals for this experiment were collected using the 6 MHz ultrasonic transducer.

#129372 - $15.00 USD Received 1 Jun 2010; revised 12 Aug 2010; accepted 14 Aug 2010; published 23 Aug 2010

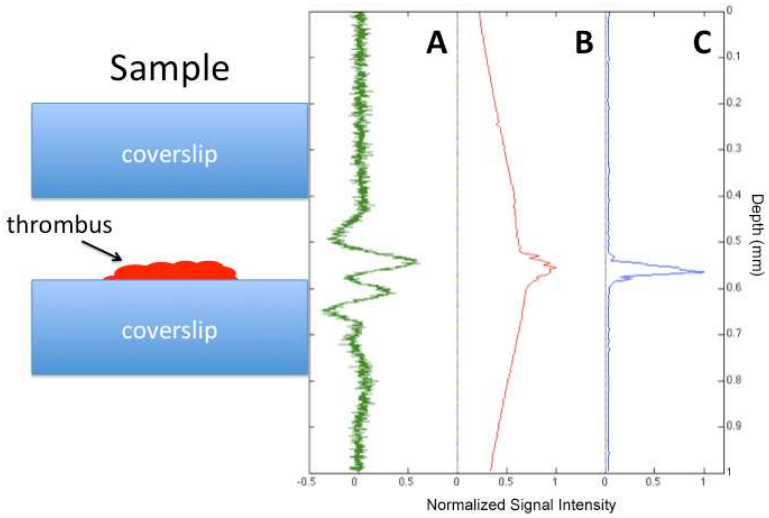

Fig. 3. Axial scans through the thrombus sample. Cartoon of sample to left. A) Photoacoustic microscopy A-line. Nominal axial resolution is 300 μm. B) Integrated photoacoustic signal, analogous to single photon fluorescence microscopy. No axial sectioning ability. C) TAUM axial line, analogous to multiphoton microscopy. Nominal axial resolution is 7 μm (twice objective Rayleigh range).

Panel A of Fig. 3 shows the depth-resolved, photoacoustic A-line of the blood sample using an Off-Axis PAM technique previously reported [15]. The axial resolution of this transducer, estimated as the speed of sound in tissue divided by the bandwidth of the transducer, is ~300 μm. Panel B shows the integrated photoacoustic signal as a function of depth. This measurement was obtained by integrating the 10 kHz harmonic photoacoustic signals over the bandwidth of the transducer, while stepping the sample through the focus of the light. As can be seen in the figure, very little sectioning is obtained from the linear photoacoustic signal due to the large wings that are present far above and below the actual position of the sample. In fact, the sectioning in panel B is clearly worse than the photoacoustic A-line in panel A. Panel C shows a TAUM A-line as a function of depth. The sharply peaked signal with no wings or background above or below the thrombus supports the conclusion that we are getting axial sectioning from the pump-probe interaction. Furthermore, the axial resolution [in Fig. 3(c)] is clearly superior to that available from traditional photoacoustic microscopy [Fig. 3(a)]. Nominally, the axial resolution in TAUM is approximately equivalent to the depth of focus, 13.4 μm.

A second experiment was performed to determine the relative signal to noise ratio (SNR) of TAUM compared to PAM. The SNR (defined as the peak signal divided by the standard deviation of the noise) was measured and compared in a sample of whole blood. The total average power on the sample was ~3 mW in both cases. One thousand pulses were used to generate the signal for both TAUM and PAM. In the PAM case, the time-domain signal was simply averaged over 1000 laser pulses. The results of these measurements yielded a TAUM SNR of 3019 and a PAM SNR of 643. This was a surprising result, given that the TAUM signal strength should be much smaller than the PAM signal strength. The explanation lies in the noise portion of the SNR equation. The variance of the noise should be proportional to the detection bandwidth. The detection bandwidth for PAM is effectively the transducer bandwidth, which is 4.78 MHz for the 6 MHz transducer. The detection bandwidth for TAUM is the total bandwidth of the sidebands used to generate the TAUM pixel, or 3.4 kHz for the

#129372 - $15.00 USD Received 1 Jun 2010; revised 12 Aug 2010; accepted 14 Aug 2010; published 23 Aug 2010

experimental conditions. We believe the ~1000 fold difference in detection bandwidth is what leads to the superior SNR of TAUM in this experiment.

As a first demonstration of TAUM imaging in a biological sample we have imaged capillaries in the cheek pouch of a Syrian hamster. For this experiment, cheek pouches were excised from freshly sacrificed Syrian hamsters. A 0.8 NA objective was used to produce a theoretical diffraction-limited transverse resolution of 0.344 μm and axial resolution of 1.87 μm. The pulse energy on the surface of the tissue was measured to be 140 nJ and 80 nJ in the pump and probe, respectively. The splitting ratio of the pump and probe beams in this experiment differ by 7.2% from the previous experiment. This discrepancy could be due to the use of different mirrors when the system was rebuilt between experiments or angle dependences in the beam splitters. The 25 MHz ultrasonic transducer was used to collect these images to take advantage of its increased bandwidth over the 6 MHz transducer used in the previous experiment. Since the transducer center frequency is not matched to the laser repetition rate, wider bandwidth leads to the measurement of more harmonics of the laser repetition frequency. Figure 4(a) shows the time-resolved photoacoustic B-scan of the capillaries in the cheek pouch. There appear to be 2 capillaries in the B-scan image; however, since the axial resolution is so poor, little else may be gleaned from the image. Figure 4(b) shows a 300-μm portion of the B-scan in Fig. 4(a), centered around the capillaries. The extracted portion was stretched in the axial dimension to provide a 1:1 scale with the 100 μm x 100 μm TAUM image, which is shown in Fig. 4(c). Figure 4(c) shows a cross-sectional TAUM image clearly resolving 3 capillaries in the hamster cheek pouch. The capillary at the right edge of the image was not apparent in the B-scan. The largest feature (FWHM) in the image is ~10 μm, which is consistent with the diameter of red blood cells. Two of the capillaries in the cross-section are elliptical, which is a result of the red blood cells not being oriented normal to the image plane.

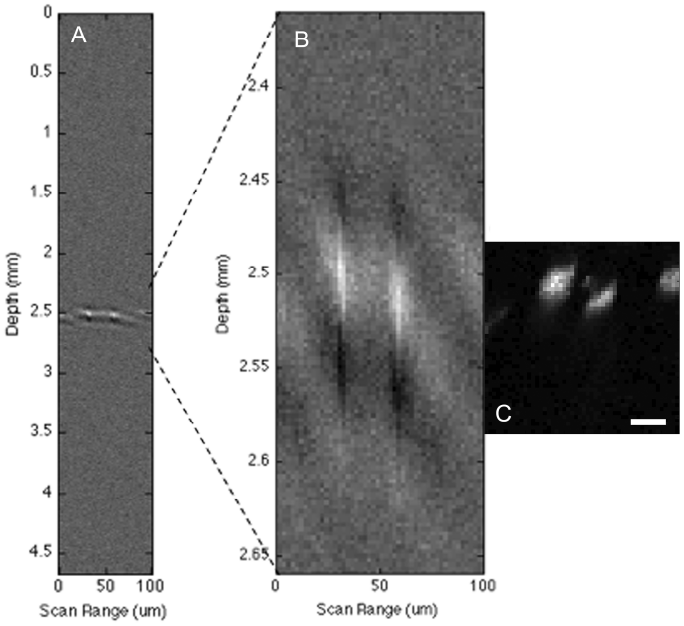

Fig. 4. , Ex vivo images of capillaries in the cheek pouch of a Syrian hamster. A) Photoacoustic B-scan (cross-section) of capillaries. B) 300 μm inset of B-scan to display 1:1 ratio with TAUM image. C) TAUM image of capillaries (cross-section) showing 3 capillaries of varying orientations. The scale bar is 20 μm.

#129372 - $15.00 USD Received 1 Jun 2010; revised 12 Aug 2010; accepted 14 Aug 2010; published 23 Aug 2010

It is important to note that the TAUM image was taken with a transducer that has a nominal axial resolution of 150 μm in the off-axis configuration, which is larger than the entire field of view of the image. While the theoretical axial resolution has not been explicitly demonstrated, Fig. 4(c) shows a minimum axial feature of 6 μm (FWHM), which is a 25-fold improvement over the axial resolution available from the single photon photoacoustic signal and over a factor of 2 better than any single photon photoacoustic microscope reported in the literature. The TAUM image in Fig. 4(c) is under-sampled (2 μm x 2 μm) in both the lateral and axial dimensions. This is due to the imaging speed restrictions imposed by the oscilloscope used to collect the TAUM signals; however, this image clearly demonstrates the increased sectioning ability of the transient absorption technique.

The primary drawback to using this frequency domain collection technique is the cost on imaging speed. The photoacoustic emission from a number of laser pulses must be collected in order to perform the frequency domain analysis noted above to extract the TAUM signal. For the experiments outlined in this paper, 1000 laser pulses are used for each pixel. In Fig. 4(c), the maximum SNR is ~200. Clearly, we could afford to sacrifice some of the SNR by reducing the number of laser pulses to improve imaging speed.

The imaging speed of the current system (~0.5 Hz) is limited by the data transfer from the digital oscilloscope to the PC rather than the number of laser pulses. With a better A/D card, the imaging speed would only be limited by the repetition rate of the laser. Therefore, for the same number of collection cycles, the imaging speed could be increased to ~10 Hz. This 20-fold increase would put this system's imaging speed on par with current photoacoustic microscopes boasting comparable lateral resolution [16]. However, it is important to note that due to the high resolution in the axial dimension, two-dimensional images will require two-dimensional scanning, as will be the case with any photoacoustic system utilizing highly focused excitation light.

The imaging speed may be further improved by integrating a higher repetition rate laser. Actively Q-switched lasers with similar or shorter pulse duration to the laser used in this study are commercially available with repetition rates up to 100 kHz. Utilizing these types of lasers would allow for increased speed or SNR, depending on the requirements of the application. While using higher repetition rate lasers will allow faster imaging speeds, the benefits are not limitless. As the pulse repetition period approaches the state recovery time [τ in Eq. (3)], the ground state population will not entirely recover between laser pulses, effectively diminishing the TAUM signal. A laser source with a pulse repetition rate of 100 kHz (10 μs period) should work well for molecules with $\tau < 3$ μs.

Potential tissue damage is always a concern for high resolution imaging due to tight focusing, especially for techniques that deposit energy into the tissue. We can use the ANSI standards for the safe use of lasers as a guide. The ANSI standards specify the maximum surface fluence. At a tissue imaging depth of 100 μm in the Syrian hamster, the surface fluence (combined pump and probe) was 4 mJ/cm^2. The ANSI maximum permissible exposure is 20 mJ/cm^2 for visible light. At an imaging depth of 100 μm, the fluence used here is at least a factor of 5 below the ANSI limit. The maximum optical fluence at the focal plane was 42.7 J/cm^2, assuming no optical losses in the tissue. While the maximum fluence is high, it is within an order of magnitude of the fluence used in recent single photon photoacoustic studies [7]. During the experiments there were no visible signs of tissue damage. It is clear from the SNR in the TAUM image [Fig. 4(c)] that the optical pulse energy could be reduced significantly, while maintaining acceptable SNR. Additionally, optimizing transducer parameters (larger transducer element size and NA for increased sensitivity) will significantly reduce the required fluence for this technique.

4. Conclusion

In conclusion, we have developed an imaging technique combining the exquisite spatial resolution afforded by non-linear microscopy with the superior penetration depth and

#129372 - $15.00 USD Received 1 Jun 2010; revised 12 Aug 2010; accepted 14 Aug 2010; published 23 Aug 2010

molecular contrast inherent to photoacoustic imaging. The result, Transient Absorption Ultrasonic Microscopy, has been used to image microvasculature in the hamster cheek pouch, demonstrating an axial resolution of at least 6 μm. To the best of our knowledge, this is the first time that an axial resolution less than 15 μm has been demonstrated in photoacoustic microscopy. These results suggest that TAUM has the potential for cellular/subcellular resolution photoacoustic imaging.

Acknowledgements

The authors would like to thank Brett Trevor at Textronix, Inc. for his help with the data acquisition hardware. This work was supported in part by a grant from the National Institutes of Health, R21EB007729.

#129372 - $15.00 USD Received 1 Jun 2010; revised 12 Aug 2010; accepted 14 Aug 2010; published 23 Aug 2010